

MOLECULAR BEAM/MS OF SILANE-HYDROCARBON OXIDATION
IN A DISCHARGE-FLOW REACTOR

G. L. Pellett and B. R. Adams

Hypersonic Propulsion Branch
High-Speed Aerodynamics Division

NASA Langley Research Center
Hampton, Virginia 23665

Paper WPA-11

Presented at the 33rd Annual Conference on Mass Spectrometry
and Allied Topics

Sponsored by American Society for Mass Spectrometry,
East Lansing, Michigan

May 26 - 31, 1985
San Diego, California

Recent results are presented from low-pressure DFR/MB/MS studies of Cl-atom initiated oxidation of He-diluted silane, silane-methane, and silane-ethylene mixtures. Research objectives have been to obtain direct evidence of free radical and molecular chain intermediates, and to determine if reaction pathways for simultaneous oxidation of silane and simple hydrocarbons (HC's) interact significantly. From the standpoint of scramjet (supersonic combustion ramjet) propulsion we need to understand the effects of premixing (vs. staged injection) of pyrophoric ignition aids, such as silane, with much lower reactivity HC's. Dilution of pyrophorics using HC's has been proposed as a means of simplifying fuel handling systems and reducing safety hazards while still retaining acceptable ignition and flameholding characteristics in subscale scramjet combustors.

Experimentally, Cl-atom, produced by microwave discharge through He-diluted Cl_2 (0.6 %) mixtures, was reacted with mixtures of He-diluted silane, or HC, or both at 1.8 torr in a 45 cm long, 2.1 cm diameter, pyrex reactor. The present work differs from our previous study (Proc. 32 nd Annual ASMS Conf.) in that (1) silane is reacted at lower pressure (1.8 vs. 3.5 torr), for shorter times (13 vs. 20 ms), and with reduced wall interaction; and (2) silane is reacted simultaneously with HC's, rather than sequentially as before. This approach led to improved free radical detection, resolution of faster reactions, and more favorable conditions for observing competitive silane/HC destruction.

Argon tracer and three selected masses were typically monitored simultaneously at 20 eV. Repetitive (4000) digital averaging of the modulated analog outputs, from the quadrupole-MS/chopped-MB system, was utilized for both microwave-ON and -OFF conditions. Data from over 600 runs were obtained for various ions as functions of silane (or HC) input flowrate (std. cc/min) under standard reaction conditions, defined in Fig. 1.

Silane consumption (percent and absolute) by Cl-atom is shown in Fig. 2; an asymptote of 4.25 SCCM silane is consistent with 50% overall Cl-atom efficiency, based on assumed 1:1 reaction. Consumptions for methane and ethylene are compared with silane results in Figs. 3 and 4. Note that addition of substantial ethylene to silane (dark symbols) had little effect on silane consumption but significantly decreased ethylene consumption. Additional results from silane-methane and -ethylene mixtures are summarized in Fig. 5. Clearly, the presence of substantial HC had little effect on silane consumption, but HC consumptions were about 10 times smaller than normal until silane was nearly exhausted. Silyl and SiH radicals are attributed primarily to "excess" ion ratios (microwave-ON) in Fig. 6. Percent excess data for silyl radical from silane and silane-HC mixtures, Fig. 7, indicate that silyl radical concentrations were large, at high silane consumptions, and unaffected by presence of either HC. Methyl radical and Cl-atom data, Figs. 8 and 9, apply only for Cl-atom attack on He-diluted methane. Note that day-to-day reproducibility on the above data was generally quite good despite presence of surface reactions.

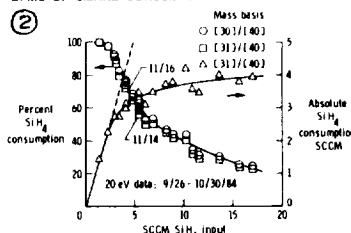
Second order kinetics plots are shown for the early phases of Cl-atom attack on silane, ethylene, and methane, Fig. 10-12. The rate coefficient for methane agrees closely with a carefully evaluated consensus k (NASA 1979). By comparison, $k(\text{Cl}+\text{SiH}_4)$ is 60 times larger than $k(\text{Cl}+\text{CH}_4)$ and 30 times larger than $k(\text{Cl}+\text{C}_2\text{H}_4)$. Finally, the relative quantities of ions associated with disilane production/destruction are constant with added silane, Fig. 13, and the resultant mass distribution is virtually identical with our previous determination, Fig. 14.

In conclusion, the rate coefficient data indicate that silane destruction by Cl-atom attack is respectively 60 and 30 times faster than for methane and ethylene, under identical conditions. Neither silyl radical concentration nor silane consumption are affected much by the presence of substantial HC, but consumption of the respective HC's is significantly inhibited until the silane is almost entirely consumed. In the case of methane this inhibition may result in part from H-atom exchange reactions; e.g., which reform $\text{CH}_4 + \cdot\text{SiH}_3$ from reaction of SiH_4 with initially-generated $\cdot\text{CH}_3$. Similar processes may occur with ethylene, but in both cases the large difference in reactivity makes it difficult to assess quantitatively the relative importance of H-atom exchange processes during simultaneous decomposition. Nevertheless, for applications which involve competitive reactions leading to ignition, it appears that decomposition of silane and HC's should not be assumed independent processes, and that chemical kinetic modelling should include H-atom exchange pathways. Further efforts in this laboratory are planned at elevated temperatures.

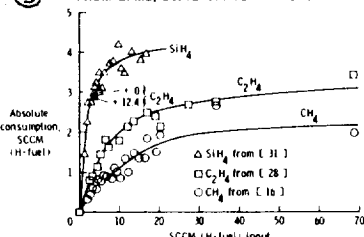
① STANDARD REACTION CONDITIONS (SRC)

SCCM: 4.25 Cl_2 : 1700 He: 14.3 Ar
 React: 13 ms; 1.8 torr; 298°K
 50% Cl-atom efficiency
 21 mm i.d., 45 cm long reactor

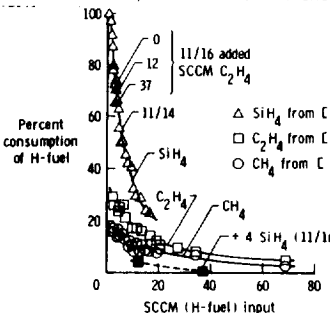
② DFMS OF SILANE CONSUMPTION BY Cl-ATOM AT SRC



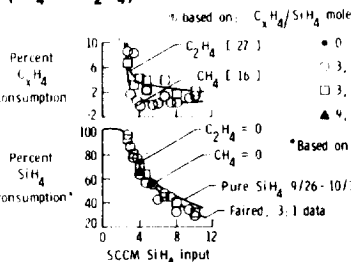
③ COMPARISON OF SiH_4 , CH_4 AND C_2H_4 CONSUMPTION FROM DFMS, USING Cl-ATOM AT SRC



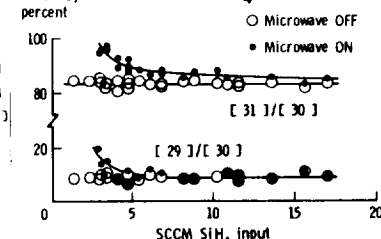
④ SiH_4 , CH_4 AND C_2H_4 CONSUMPTION FROM DFMS, USING Cl-ATOM AT SRC



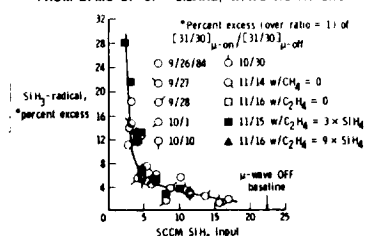
⑤ COMPETITIVE CONSUMPTION OF SiH_4 + (CH_4 OR C_2H_4) MIXTURES, USING Cl-ATOM



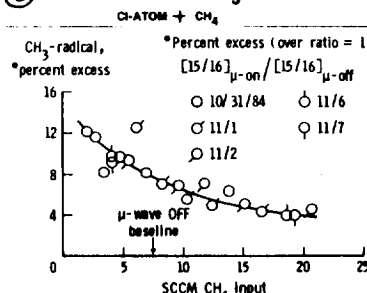
⑥ PRODUCTION OF SiH_x RADICALS FROM Cl + SiH_4 AT SRC



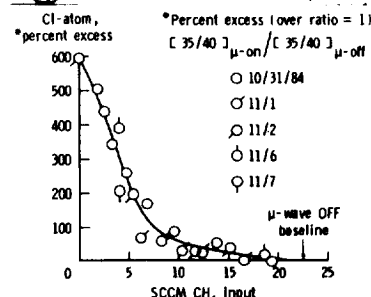
⑦ PRODUCTION OF SiH_3 RADICAL W/O PRESENCE OF HC FROM DFMS OF Cl + SILANE, W/O HC AT SRC



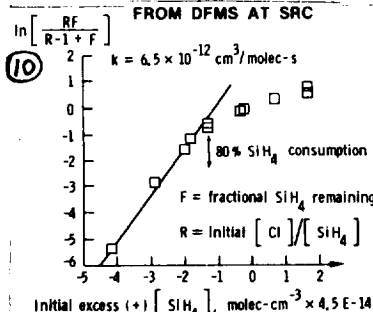
⑧ PRODUCTION OF CH_3 RADICAL



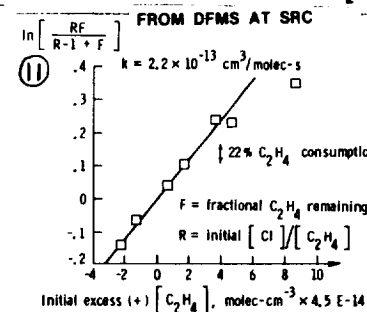
⑨ DESTRUCTION OF Cl-ATOM BY CH_4



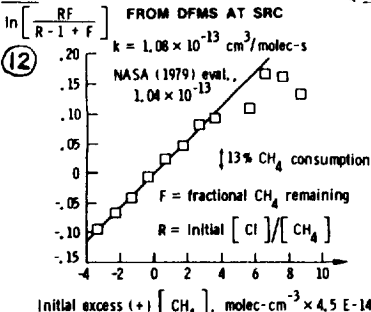
SECOND ORDER KINETICS FOR Cl + SiH_4 FROM DFMS AT SRC



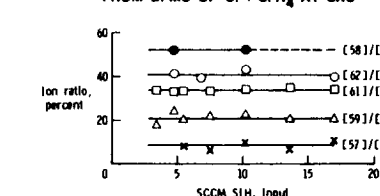
SECOND ORDER KINETICS FOR Cl + C_2H_4 FROM DFMS AT SRC



SECOND ORDER KINETICS FOR Cl + CH_4 FROM DFMS AT SRC



⑬ MASS ABUNDANCE OF DISILANE SPECIES FROM DFMS OF Cl + SiH_4 AT SRC



⑭ MASS DISTRIBUTION OF DISILANE SPECIES FROM DFMS OF SiH_4 + Cl-ATOM AT SRC

